Research Square

Preprints are preliminary reports that have not undergone peer review.
They should not be considered conclusive, used to inform clinical practice,
or referenced by the media as validated information.

From Flower Bud to Flowering: A Comprehensive Study on the Sexual Reproductive Development Characteristics of the Oil Tree Species Idesia polycarpa

qimei Wang
Guizhou University
chao Gao
gaochao@gzu.edu.cn

Guizhou University
fuhua Fan
Guizhou University
qiling Song
Guizhou University
xianqin Wan
Guizhou University
xudong Zhao
Guizhou University
feifei Li
Guizhou University

Research Article

Keywords: Idesia polycarpa, dioecious, flower bud differentiation, gametophyte development, pollen viability, flower-visiting insects

Posted Date: July 9th, 2026

DOI: https://doi.org/10.21203/rs.3.rs-10139252/v1

License: This work is licensed under a Creative Commons Attribution 4.0 International License.
Read Full License

Additional Declarations: No competing interests reported.

Abstract

Idesia polycarpa is an important native woody oil tree species in China, yet its dioecious reproductive system hinders elite variety breeding and yield improvement. Here, we systematically investigated its reproductive developmental characteristics using paraffin sectioning, scanning electron microscopy, pollen viability assays, and field observations, covering flower bud differentiation, megasporogenesis/microsporogenesis, gametophyte development, and flowering biology. Results showed: (1) Flowering occurs from late April to early May, with bud differentiation divided into seven stages. Abortive organ degeneration in female and male plants occurs at megaspore and microspore mother cell stages, respectively. (2) Male flowers produce functional pollen with a polar/equatorial ratio of 2.61 (perprolate); anthers dehisce longitudinally with lipid droplets along slit margins. Female flowers possess a wet stigma, superior ovary with parietal placentation, and anatropous ovules; embryo sac development follows the Polygonum type. (3) MTT and TTC were the most suitable pollen viability assays, with viability at full bloom reaching 53% and 39%, respectively. Pollen tubes germinate within 4 h and reach the ovary base within 72 h after artificial pollination. (4) An outcrossing index of four confirms obligate xenogamy, with eight insect species (including *Apis cerana cerana* and *Bombus* spp.) as principal pollinators. This study provides a theoretical basis for early sex identification, elite breeding, artificial pollination, and high-yield cultivation of *I. polycarpa*.

1 Introduction

Idesia polycarpa (Salicaceae) is an important woody oil tree species native to Asia and widely distributed in China, Korea, and Japan[1][2]. In China, it is mainly found in the trans-subtropical and warm-temperate regions south of the Qinling Mountains and Huaihe River. The species exhibits several advantageous traits, including rapid growth, high yield, tolerance to cold and drought, strong adaptability, and sustained high fruit production even in trees over 100 years old[3]. It is therefore suitable for both oil and timber production. The fruits of *I. polycarpa* are characterized by high oil content, with pulp oil content ranging from 8.38% to 48.35% and seed oil content from 12.6% to 28.17%, earning the species the reputation of a “tree oil depot”[4][5]. The oil is rich in unsaturated fatty acids, with linoleic acid accounting for up to 81.74%. Linoleic acid is an essential fatty acid that can only be obtained through the diet or dietary supplements[4]. In addition, the oil contains natural antioxidants and various bioactive compounds, including tocopherols, phytosterols, and polyphenols, which possess free-radical scavenging activity and are beneficial to human health. Owing to its high nutritional value, the oil can be used as a high-quality edible oil[6][7][8]. In terms of comprehensive resource utilization, *I. polycarpa* has broad application value in food, hygiene, medicinal functions, and as a raw material for biodiesel[6]. In recent years, *I. polycarpa* oil has also attracted attention as a potential feedstock for specialty resins and biodiesel[6][9]. Therefore, in-depth research on this species is important not only for the utilization of specific resources but also for understanding and conserving the biodiversity of related woody oil plants.

For perennial woody plants, sexual reproduction provides the biological foundation for population persistence, maintenance of genetic diversity, and yield formation. Flower bud differentiation determines the initiation of yield formation, whereas the development of male and female gametophytes is essential for sexual reproduction and seed production. Cytological studies can provide morphological markers for early sex identification, which is critical for the breeding and cultivation management of dioecious plants[10][13]. In addition, reproductive biological traits, including flowering phenology, pollen viability, pollination mode (wind/insect), synchrony of male and female flowering, and effective pollinator species, collectively determine male-to-female ratios and pollination management strategies in natural and plantation forests, thereby directly influencing reproductive strategies, population dynamics, and genetic structure. These factors are also central to overcoming the bottleneck of low yield[14][15]. Therefore, a systematic investigation of the reproductive biology of *I. polycarpa* provides a theoretical basis for understanding its population biological characteristics, conducting cross-breeding, and improving cultivation practices.

Current research on *I. polycarpa* has primarily focused on fruit oil processing, omics analyses, and artificial fatty acid synthesis. Existing studies have systematically examined variations in oil content and physicochemical properties, oil dynamics during harvesting, optimization of extraction processes, and the expression regulation of key genes such as SAD, FAD2, and PDAT[16]. In contrast, research on reproductive biology, which underlies yield determination, remains relatively limited. Preliminary studies have divided flower bud differentiation into six stages and described the morphological abortion of floral organs[17][18]. However, systematic investigations integrating the internal regulatory mechanisms of flower bud differentiation and dormancy, the complete cytological processes of male and female gametophyte development, and their molecular basis are still lacking[19]. More importantly, studies on flowering phenology, pollination vectors, and fruit-set limiting factors that directly influence fruit production are almost absent. This lag in reproductive biology research has severely constrained efficient breeding strategies, such as early sex identification and shortening of the juvenile phase, as well as scientific cultivation practices, including rational allocation of male and female plants and flowering period management. Accordingly, the present study systematically investigated the major reproductive developmental processes of *I. polycarpa* from flower bud formation to anthesis from a reproductive biology perspective. By integrating ontogenetic, histological, and phenological analyses, the study focused on flower bud differentiation, male and female gametophyte development, and flowering and pollination characteristics. Cytological observations combined with phenological investigations were used to elucidate the key events and morphological markers of reproductive development and to evaluate the synchrony of flowering periods and pollination modes between male and female plants. This study provides a theoretical basis for early sex identification, understanding reproductive ecology, regulation of flowering periods, and high-yield cultivation of *I. polycarpa*, thereby promoting the sustainable utilization and scientific conservation of this species.

2 Materials and Methods

2.1 Study site and plant materials

The study site was located at the *I. polycarpa* research base of Guizhou University (107°13'52"E, 26°35'00"N) at an altitude of 1100 m. The region has a mid-subtropical monsoon humid climate, with an annual mean temperature of 15.5°C, a frost-free period of 289 days, annual mean precipitation of 1084.8 mm, and an average relative humidity of 78%. Rainfall and heat occur during the same season. The experimental materials consisted of 8-year-old adult *I. polycarpa* seedling trees with an average height of approximately 3 m, moderate vigor, and healthy growth. Conventional soil, water, and fertilizer management practices were applied. The plant materials used in this study were exclusively obtained from this cultivated base, which is managed by our research group, and were not collected from the wild; therefore, no specific collection permits were required. Formal taxonomic identification of the species was performed by Professor Xinxiang Bai from the College of Forestry, Guizhou University. Voucher specimens (specimen No. GZAC0015823) have been deposited at the Herbarium of the College of Forestry, Guizhou University (GZAC). All experimental research on plant materials in this study complies with institutional, national, and international guidelines.

2.2 Observation of flower bud differentiation

Fifteen female and fifteen male plants with uniform growth vigor were selected and labeled as experimental materials. Observations were conducted over two growth cycles from 2024 to 2025. Every 15 days, three terminal buds were collected from each of the four directions (east, south, west, and north). After leaf expansion, flower buds were sampled every 5 days. The sampled flower buds were photographed and immediately fixed in Carnoy's fixative (ethanol:glacial acetic acid = 3:1), then transferred to 70% ethanol and stored at 4°C. All fixed materials were used for morphological and histological observations of inflorescence buds and flowers.

2.3 Histological observation of megaspores, microspores, and male/female gametophytes

Collected and fixed inflorescences and flower buds from female and male plants were stained with hematoxylin for 2–3 days and then rinsed under running water for 12 h for bluing. The samples were subsequently dehydrated through a graded ethanol series, cleared with xylene, infiltrated with paraffin, and embedded. Sections of 8–10 μm thickness were prepared using a rotary microtome (Leica, RM2235, Germany), mounted on slides, deparaffinized, and sealed with neutral balsam[20]. Observations and image acquisition were conducted using a biological microscope (Olympus, BX53(LED), Japan).

2.4 Observation of flowering phenology and floral organs

2.4.1 Flowering phenology observation

Flowering phenology of *I. polycarpa* was observed and recorded continuously for two consecutive years from 2024 to 2025. The recorded stages included initial flowering (approximately 10% of flowers open),

full bloom (approximately 30%–75% of flowers open), and final flowering (when most flowers had fully opened).

2.4.2 Stereomicroscopy and scanning electron microscopy (SEM) observation of floral organs

During the full-bloom stage of female and male *I. polycarpa* plants, fresh pollen, stigma, and style samples were collected for observation and imaging using a stereomicroscope and a scanning electron microscope. Before SEM observation, the samples were coated with a thin layer of gold-palladium (Au-Pd) using an ion sputter coater (MSP Mini, USA). Coating was performed under a vacuum of approximately 10 Pa with a sputtering current of 20 mA for 30 s to improve sample conductivity. The treated samples were then observed using a scanning electron microscope (Hitachi, TM4000 Plus, Japan) at an accelerating voltage of 5.0 kV. Morphological characteristics were documented by SEM imaging, and the length and width of ovules, pollen grains, and stigmas were measured directly from the digital images using the accompanying software.

2.5 Pollination characteristics

2.5.1 Screening of pollen viability staining methods

During the full-bloom stage, normally developed pollen was collected from male *I. polycarpa* plants. Four staining methods—acetic carmine, I_2-KI, TTC, and MTT—were used to evaluate pollen viability based on specific color reactions[21] in order to determine the most suitable method. Each method was repeated three times, and five random fields of view were examined in each replicate (≥ 30 pollen grains per field).

2.5.2 Fluorescence microscopy observation of pollen tubes

On the day of anthesis, female flowers were emasculated and pollinated on the stigma using normal pollen with high viability collected from male plants. The flowers were then bagged for observation. Female pistils were sampled at 1, 2, 4, 8, 12, 24, 48, and 72 h after pollination. Care was taken to preserve the integrity of the stigma structure. After fixation for 5 h, the samples were stored in 70% alcohol. The samples were rehydrated through a graded ethanol series, softened in 8 mol/L NaOH for 8 h, and then soaked overnight in distilled water. Subsequently, they were stained with 0.1% aniline blue solution prepared in 0.15 mol/L K_2HPO_4 for 3–4 h[22]. Following routine squashing, the samples were observed and photographed under a fluorescence microscope (OLYMPUS, BX53(LED), Japan) to document pollen germination on the stigma and the dynamics of pollen tube growth within the style.

2.6 Flower-visiting insect survey

During the full-bloom period of female and male plants, systematic observations were conducted on sunny days with calm or light wind conditions from 8:00 to 17:00 daily. Observations continued for 3–5 consecutive days. For each observation period, the species of flower-visiting insects, visiting duration, and behavioral characteristics, including the type of flower visited (female or male), were recorded. A

digital camera was used for documentation, and unidentified insect species were safely captured and preserved as specimens for subsequent identification when necessary.

2.7 Estimation of the outcrossing index (OCI)

Floral traits of *I. polycarpa* were evaluated according to the criteria of Dafni (1992) to calculate the OCI[23]: (1) flower/inflorescence diameter: <1 mm = 0; 1–2 mm = 1; 2–6 mm = 2; >6 mm = 3; (2) time interval between anther dehiscence and stigma receptivity: simultaneous or protogynous = 0; protandrous = 1; and (3) spatial relationship between stigma and anthers: same height = 0; spatially separated = 1. The OCI value was calculated as the sum of the three scores. Breeding systems were classified as follows: OCI = 0, cleistogamy; OCI = 1, obligate autogamy; OCI = 2, facultative autogamy; OCI = 3, self-compatible (sometimes requiring pollinators); and OCI = 4, partially self-compatible (outcrossing requiring pollinators).

3 Results and Analysis

3.1 Process of flower bud differentiation

Flower bud differentiation in *I. polycarpa* follows a “differentiation and flowering within the same year” pattern, with the entire process lasting approximately 38 days (Fig. 1, Table 1).

Table 1
Correlation between megasporogenesis/microsporogenesis and female/male gametophyte development in I. polycarpa

2024	2025	Male flower developmental stage	Female flower developmental stage
9.01–3.05	9.08–3.08	None	None
3.06–3.16	3.09–3.18	Male inflorescence axis differentiation	Female inflorescence axis differentiation
3.17–3.26	3.19–3.28	Male flower meristem emergence	Female flower meristem emergence
3.27–4.3	3.29–4.5	Sepal primordium appearance	Sepal primordium appearance
4.4–4.7	4.6–4.10	Stamen primordium appearance	Stamen primordium appearance
4.8–4.11	4.11–4.15	Bisexual stage, both carpel and stamen primordia present	Bisexual stage, both carpel and stamen primordia present
4.12–4.15	4.16–4.18	Androecium and gynoecium formation stage (young anthers form, ovule formation)	Androecium and gynoecium formation stage (young anthers form, ovule formation)
4.16–4.18	4.19–4.20	Microspore mother cell stage, ovule abortion	Androecium and gynoecium formation stage (young anthers form, ovule formation)
4.19–4.23	4.21–4.25	Microspore mother cell meiosis	Megaspore mother cell formation
		Tetrad stage	
		Uninucleate microspore at peripheral stage	Megaspore mother cell development
4.24–4.25	4.26–4.30	Mature anther	Dyad formation (of megaspores)
4.26–5.2	4.31–5.8	Mass pollen shedding	Megaspore mother cell meiosis forming tetrad
5.2–5.8	5.9–5.12		Binucleate (embryo sac)
5.8–5.12	5.11–5.20		Eight-nucleate embryo sac
5.13–5.20	5.21–5.22		7-celled, 8-nucleate mature embryo sac

Before differentiation, male and female flower buds showed similar length and width. As development progressed, bud volume increased markedly. At the undifferentiated stage, the morphology of the inflorescence axis differed substantially between female and male buds (Fig. 1-A1, B1). During the

inflorescence primordium differentiation stage, hemispherical protrusions formed in the leaf axils (Fig. 1-A2, B2). Subsequently, sepal primordia began to differentiate, appearing as two curved protrusions surrounding the floral primordium (Fig. 1-A3, B3). As the bud scales continued to open, the inflorescence elongated significantly, with female buds elongating more rapidly than male buds. At the same time, internal stamen primordia began to differentiate, with one or two small protrusions forming between the sepals and the inner growth point (Fig. 1-A4, B4). Upon entering the bisexual stage, additional internal protrusions differentiated, and some central protrusions gradually developed into pistil primordia. At this stage, pistil primordia appeared in male flowers (staminate flowers), whereas stamen primordia appeared in female flowers (pistillate flowers), resulting in the coexistence of stamen and pistil primordia (Fig. 1-A5, B5). Following the bisexual stage, the flowers entered the stamen/pistil formation stage, during which rapid organ differentiation occurred. In male flowers, stamen primordia gradually differentiated into anthers and filaments, whereas in female flowers, pistil primordia gradually differentiated into stigmas, styles, and ovary primordia (Fig. 1-A6, B6). The subsequent stage was unisexual development. In male flowers, the differentiated pistil primordia ceased development while the stamens continued to mature; conversely, in female flowers, the differentiated stamen primordia ceased development while the pistils continued to develop. After approximately 30 days of differentiation, unisexualization was completed. At this stage, the ovary in male flowers had degenerated and collapsed, whereas the anthers developed normally (Fig. 1-A7). In female flowers, the ovules were fully developed, while the anthers had aborted (Fig. 1-B7).

3.2 Megasporogenesis, microsporogenesis, and male/female gametophyte development

3.2.1 Megasporogenesis and female gametophyte development

In female flowers, the ovule primordium developed two integuments. At the apex of the nucellus, a megaspore mother cell differentiated directly from an archesporial cell. This cell was large and spherical, with a prominent nucleus and dense cytoplasm (Fig. 2-A, B). Subsequently, the megaspore mother cell elongated and its nucleus enlarged. Following meiosis I, a dyad of megaspores was formed (Fig. 2-C). Meiosis II then produced a linear tetrad of megaspores (Fig. 2-D). Among the four megaspores, the chalazal megaspore gradually enlarged and developed into the functional megaspore (Fig. 2-E), whereas the remaining three cells gradually degenerated, exhibiting dense cytoplasm, irregular morphology, and indistinct nuclei. At this stage, a uninucleate embryo sac was formed. The nucleus of the uninucleate embryo sac was large and gradually migrated toward the center of the embryo sac, which became elongated and contained lightly stained cytoplasm (Fig. 2-F).

OI outer integument, II inner integument, Nuc nucellus, ARC archesporial cell, MMC megaspore mother cell, DM degenerated megaspore, FM functional megaspore, ES embryo sac, EC egg cell, PNC polar nuclei, SYN synergid, AC antipodal cell.

The functional megaspore underwent mitosis to form a binucleate embryo sac. As development proceeded, the binucleate embryo sac elongated further (Fig. 2-G), became vacuolated, and the two nuclei migrated toward opposite poles. Dense cytoplasm surrounded each nucleus, and cytoplasmic connections were present between them. Each of the two nuclei subsequently underwent another mitotic division, resulting in a tetranucleate embryo sac (Fig. 2-H). A further round of mitosis produced an eight-nucleate embryo sac. Rapid development at this stage made simultaneous observation of the four nuclei at each pole difficult within the same focal plane. Subsequently, one nucleus from each pole migrated toward the center to form the central cell, marking maturation of the embryo sac. The mature embryo sac was hourglass-shaped and consisted of one egg cell, two synergids, three antipodal cells, and one central cell (Fig. 2-I). At the micropylar end, three cells formed the egg apparatus, with the centrally located egg cell being larger than the surrounding synergids (Fig. 2-J). The two nuclei of the central cell were closely positioned in the center of the embryo sac (Fig. 2-K). At the chalazal end, only two antipodal nuclei were visible because one antipodal cell had degenerated (Fig. 2-L). Embryo sac development in *I. polycarpa* follows the Polygonum type, which is the most common developmental type among angiosperms. In male flowers, ovule abortion occurred at the megaspore mother cell stage, resulting in loss of ovule viability and eventual collapse into an empty, shrunken structure. The entire process of megasporogenesis and female gametophyte development lasted approximately 32 days (Table 1).

3.2.2 Microsporogenesis and male gametophyte development

When stamen primordia formed in male flowers, the epidermis consisted of uniformly sized thin-walled cells that were not yet differentiated (Fig. 3-A). Subsequently, cells at the four corners of the anther differentiated more rapidly, and the anther became four-lobed. A vascular bundle developed in the center and differentiated into the connective. At this stage, epidermal cells with larger size and nuclei than surrounding cells differentiated into archesporial cells (Fig. 3-B). The archesporial cells underwent periclinal division, giving rise to primary parietal cells and primary sporogenous cells (Fig. 3-C, D). The primary parietal cells further divided and differentiated into four anther wall layers, from the outside to the inside: epidermis, endothecium, 1–2 middle layers, and the innermost tapetum (Fig. 3-E, F). The tapetum consisted of a single layer of cells with large, densely stained nuclei, closely arranged, and of secretory type. As anther development proceeded, at the tetrad stage, the tapetal cell contents gradually decreased, and secreted substances supported microsporogenesis and development (Fig. 3-G). At the microspore stage, tapetal cells remained at the periphery and retained their secretory function (Fig. 3-H). When microspores matured (bicellular pollen stage), the tapetal cells completely underwent autolysis (Fig. 3-I). The middle layer degenerated early, separating from the tapetum at the microspore mother cell stage and beginning to disintegrate (Fig. 3-H), and it disappeared completely by the microspore stage. At the uninucleate microspore stage, endothecium cells enlarged, became vacuolated, and their radial and tangential walls elongated (Fig. 3-H). At anthesis, the inner tangential and transverse walls developed band-like fibrous thickenings. The epidermis differentiated earliest as a single layer of tightly packed cells in early development, and later became elongated and collapsed, remaining only as remnants at

anthesis (Fig. 3-J). In female flowers, after primary parietal cells further differentiated into four wall layers, anther development ceased, ultimately resulting in only shrunken anther wall remnants (Fig. 3-K, L).

In male flowers, stamens were mostly densely arranged. Microspore mother cells were significantly larger than surrounding parietal cells, with dense cytoplasm and almost no vacuoles (Fig. 4-A–C). After meiosis I, a cell wall formed between the two daughter nuclei, indicating a successive type of cytokinesis (Fig. 4-D). The resulting tetrads were tetrahedral (Fig. 4-E–G) and exhibited shallow depressions (Fig. 4-H). In contrast, in female flowers, anther development arrested at the microspore mother cell stage, and the locules eventually became dry, ruptured, and formed empty cavities (Fig. 4-L, M).

The tetrad stage was brief. Gradual dissolution of the tapetum released microspores from tetrads as uninucleate microspores, which then entered male gametophyte development. Microspores increased in volume and nuclear size, followed by cytoplasmic liquefaction, and a large vacuole formed that displaced the nucleus to one side, resulting in polarization (Fig. 4-I). Subsequently, highly asymmetric mitosis produced a large vegetative nucleus and a small generative nucleus, forming bicellular pollen grains (Fig. 4-J). Mature pollen grains contained dense cytoplasm, were rich in starch, possessed three germinal apertures, and remained in the bicellular state (Fig. 4-K). In female flowers, anther development arrested at the microspore mother cell stage, preventing male gametophyte formation (Fig. 4-O). The entire process of microsporogenesis and male gametophyte development lasted approximately 28 days (Table 1).

3.3 Flowering phenology and floral organ observation

3.3.1 Flowering phenology survey

Flowering phenology differed between male and female plants, with male flowers opening approximately 3 days earlier than female flowers. The first flowering date of the population occurred in late April, with the initial flowering stage lasting about 7 days. Full bloom occurred from May 3 to May 18, lasting approximately 7 days. The final flowering stage lasted about 6 days. The total flowering period of the population was approximately 22 days (Table 2).

Table 2
Flowering phenology of I. polycarpa

Year	first flowering date	full bloom	full bloom	total flowering period
2024	4.26–5.2	5.3–5.11	5.11–5.17	21 d
2025	4.30–5.8	5.12–5.18	5.18–5.23	23 d

3.3.2 Observation of floral organs

After winter dormancy, both female and male flowers developed rapidly in the following spring (Table 3 and Fig. 5). In pistillate flowers, the carpels converge and close above the ovary, and their extensions form curved style arms and stigma tissues, typically 5–6 in number. At anthesis, the average flower opening diameter of pistillate flowers was 10.75 × 10.68 mm. The style length was 2.55 ± 0.62 mm, and the width was 0.35 ± 0.09 mm. The styles radiate from the apex and terminate in a spherical stigma (Fig. 5-A1, A6, A7).

Table 3
Statistics of floral organ numbers in female and male flowers of I. polycarpa

Flower type	Measured indicator					
	Measurement Parameter	Minimum (mm)	Maximum (mm)	Mean (mm)	SD	Number of Samples (Flowers)
Female flower	Petal length	4.02	6.88	5.06	0.98	30
	Petal width	1.93	4.24	3.10	0.87	30
	Filament length	0.47	2.98	1.24	0.90	30
	Filament width	0.03	0.12	0.06	0.03	30
	Ovary size	3.14	4.29	3.59	0.38	30
	Ovary width	2.29	3.97	2.92	0.57	30
	Style length	1.50	3.44	2.55	0.62	30
	Style width	0.19	0.47	0.35	0.09	30
	Diameter of the fully opened flower	9.81×9.15	12.17×13.61	10.75×10.68	0.82×1.31	30
Male flower	Petal length	4.49	8.23	6.974	0.36	30
	Petal width	2.73	4.22	3.723	0.15	30
	Filament length	4.23	11.83	5.978	0.70	30
	Filament width	0.1	0.22	0.137	0.01	30
	Rudimentary ovary	0.82	2.16	1.639	0.14	30
	Style width	0.31	1.32	0.634	0.09	30
	Diameter of the fully opened flower	13.43×12.86	21.4×23.71	15.82×16.64	0.73×1.07	30

The stigma measured 312.12–462.20 μm in length and 570.30–596.20 μm in width, with abundant secretions, indicating a wet stigma type (Fig. 5-A9, A10). The ovary had parietal placentation, was superior, and measured 3.59 ± 0.38 mm in length and 2.92 ± 0.57 mm in width (Fig. 5-A1, A6, Table 3). The ovule was anatropous, with a length of 392.78–420.03 μm and a width of 203.24–256.74 μm. At this stage, the anthers of pistillate flowers were completely empty and lacked pollen (Fig. 5-A5).

In male plants, staminate flowers resumed growth and increased in size (Fig. 5-B1, B6, B7). At flowering, the central anthers dehisced first, and by full bloom, the entire male flower was fully open. The filament length was 5.98 ± 0.70 mm, and the width was 0.14 ± 0.01 mm, with all anthers forming a dome-like structure. The average flower opening diameter was 15.8 × 16.6 mm. The anthers were bright yellow, conspicuous, and dehisced longitudinally to release pollen, with lipid droplets present along the slit margins (Fig. 5-B7, B8). Anther length ranged from 989.74 to 1160.44 μm, and width ranged from 876.70 to 959.53 μm. The pollen grains observed in equatorial and polar views (Fig. 5-C1, C2) were perprolate. The polar axis (P) ranged from 21.76 to 24.91 μm (mean 22.63 μm), and the equatorial axis (E) ranged from 7.50 to 10.28 μm (mean 8.85 μm), with a P/E ratio of 2.42–2.90 (mean 2.61). In polar view, pollen grains were trilobed and nearly circular, with three colpate germinal furrows. The colpus length ranged from 18.20 to 20.24 μm, with a mean of 19.28 μm. The exine exhibited honeycomb-like sculpturing with thickened margins. Overall, normal pollen grains were plump and regular, whereas aborted pollen grains (Fig. 5-B10) were shrunken, collapsed, and irregular in shape. At anthesis, ovules in staminate flowers were already desiccated, and the stigma was dry and yellow (Fig. 5-B2, B5).

3.4 Pollination characteristics

3.4.1 Screening of pollen viability staining methods

Functional pollen from male plants was stained using acetic carmine (Fig. 6-A), TTC (Fig. 6-B), I_2-KI (Fig. 6-C), and MTT (Fig. 6-D). The results showed that acetic carmine stained all pollen grains red, leading to an overestimation with no meaningful reference value. With TTC staining, strongly viable pollen appeared red, weakly viable pollen appeared light red or pink, and non-viable pollen remained colorless; the measured viability was 39%. With I_2-KI staining, only a few pollen grains stained black, while most remained colorless; therefore, this method could not reliably assess the pollen viability of *I. polycarpa*. With MTT staining, strongly viable pollen appeared deep blue–purple; lower viability corresponded to lighter staining, and non-viable pollen remained colorless; the measured viability was 53%. Therefore, TTC and MTT staining were identified as the most suitable methods for assessing pollen viability in *I. polycarpa*.

3.4.2 Fluorescence microscopy observation of pollen tubes

The fluorescence microscopy results of styles at different time points after artificial pollination in female *I. polycarpa* plants are shown in Fig. 7. At 1–2 h after pollination, almost no germination was observed (Fig. 7-A, B). At 4 h, pollen began to germinate abundantly, and pollen tubes penetrated the stigma (Fig. 7-C). At 8 h, pollen tubes had deeply penetrated the stigma and continued to elongate (Fig. 7-D). At 12 h, pollen tubes showed further elongation (Fig. 7-E). At 24 h, pollen tubes reached the middle of the style, with lengths of 542.79–680.65 μm (Fig. 7-F). At 48 h, numerous pollen tubes were present in the style, reaching the lower middle region, with lengths of 567.86–869.02 μm (Fig. 7-G). At 72 h, pollen tube length reached 2311.12–3991.68 μm, with a mean of 2871.68 μm, and pollen tubes had reached the ovary (Fig. 7-H).

3.4.3 Flower-visiting insect survey

In the study of flower-visiting insects of *I. polycarpa*, the visitor community was diverse. A total of 8 insect species from 3 orders and 6 families were recorded (Fig. 8, Table 4). Hymenopterans, particularly Apis cerana cerana and Bombus spp., were identified as the primary pollinators (Fig. 8-A, B). Apis cerana cerana was the main daytime visitor, with activity peaks corresponding to the main flowering period of *I. polycarpa* in the morning (9:00–11:00) and afternoon (14:00–16:00). Its foraging behavior involved sequential visits to 3–5 flowers on the same inflorescence, spending approximately 15–25 s per flower. While collecting nectar, its thorax and legs frequently contacted the stamens. It visited both female and male flowers and effectively transferred pollen to stigmas. Bombus spp. were mainly active in the early morning (8:30–10:30) and late afternoon (15:00–17:00), with longer single-flower visitation durations (20–30 s). Due to their larger body size, bumblebees made more extensive contact with floral structures and carried more pollen per visit. Their foraging range was significantly larger than that of honeybees; they often visited 2–3 different plants within a single foraging bout. Bumblebees visited both female and male flowers, with afternoon activity mainly focused on female flowers, and they effectively transferred pollen to stigmas.

Table 4
Flower-visiting insect survey sheet

Number	Species name	Family	Order
1	*Apis cerana cerana*	Apidae	Hymenoptera
2	*Bombus* spp	Apidae	Hymenoptera
3	*Chelidonium argentatum*	Cerambycidae	Coleoptera
4	*Formicidae*	Formicidae	Hymenoptera
5	*Harmonia axyridis*	Coccinellidae	Coleoptera
6	*Coccinella septempunctata*	Coccinellidae	Coleoptera
7	*Rhyncomya inconspicua*	Rhiniidae	Diptera
8	*Lucilia sericata*	Calliphoridae	Diptera

Ants were nectar-feeding insects and were abundant in number; however, due to their small body size, prolonged residence on the same inflorescence, and limited mobility, although they visited both female and male flowers, they were rarely able to achieve effective cross-pollination between female and male plants (Fig. 8-D). Dipterans frequently visited male flowers but rarely visited female flowers. Although a relatively large amount of pollen adhered to their body hairs, their species diversity and individual abundance were low; they could contribute to pollination but played only a minor role (Fig. 8-G, H). Coleopterans often rested on male flowers during visits; their smooth body surfaces were not conducive to pollen adherence, and they were not observed visiting female flowers. In addition, they tended to damage floral structures during visitation, making them unfavorable for pollination (Fig. 8-C, E, F).

3.5 Estimation of the outcrossing index (OCI)

The evaluation of the breeding system of *I. polycarpa* based on Dafni's outcrossing index (OCI, 1992) is shown in Table 5. Male flower diameter was 15.7 mm, and female flower diameter was 10.7 mm, both > 6 mm, yielding a score of 3. The time interval between anther dehiscence and stigma receptivity was 0, as the female stigma was already receptive at the time of male anthesis. The plants are dioecious, with spatial separation, yielding a score of 1. The total OCI was 4, corresponding to an "obligate outcrossing" system. Thus, *I. polycarpa* requires pollen from another individual as a pollen source, and pollination depends on external vectors.

Table 5
The out-crossing index of I. polycarpa

Observation index	Outcome	Observation value
Flower diameter	> 6mm	3
Time interval between pollen dispersion from anther and stigma receptivity	Protogyny	0
Spatial relationship between stigma and anther	Stigma higher than anther	1
OCI value	4	

4 Discussion

Understanding flowering biology and ontogeny, including key stages of flower bud differentiation, is helpful for reproductive regulation. Flower bud morphogenesis in trees is essential for fruit quality and yield. In recent years, research on flower bud differentiation in dioecious plants has advanced. Through morphological and anatomical observations, it has been found that the proportion of flower bud differentiation in short-branch terminal buds of male *I. polycarpa* plants is the highest, reaching 76.3%, and that both male and female flowers form unisexual flowers through selective abortion[2]. A study using male plants derived from the cross between kiwifruit (*Actinidia chinensis*) 'Jinli' and 'Moshan 4' systematically evaluated the variation and diversity of floral traits and pollen germination rates, and selected lines that could serve as excellent pollinating varieties, providing a material basis for male line selection in dioecious fruit trees[24]. Some research has divided flower bud differentiation in *I. polycarpa* into six stages: undifferentiated stage, differentiation stage, inflorescence axis differentiation stage, inflorescence differentiation stage, floral organ differentiation stage, and stamen/pistil differentiation stage[25]. However, based on classification criteria used for many dioecious plants and our observed structures, this study defined the protrusion in the leaf axil as the initial sign of flower bud morphogenesis and redefined flower bud differentiation in *I. polycarpa* into seven stages: undifferentiated stage, inflorescence primordium differentiation stage, sepal primordium differentiation

stage, stamen primordium differentiation stage, bisexual stage, stamen/pistil differentiation stage, and unisexual completion stage. The inflorescence primordium differentiation stage is the turning point at which the plant transitions from vegetative growth to reproductive growth, marking a shift from simple increases in volume and leaves to a development phase centered on reproduction. Therefore, defining this as the starting point of flower bud differentiation is more conducive to understanding the plant's growth process and predicting the flowering period. In the dioecious plant *Actinidia chinensis*, the sex-determining role of this differentiation stage (inflorescence primordium differentiation) has also been systematically verified at the molecular level. Akagi et al. (2018) found that the Shy Girl protein encoded on the kiwifruit Y chromosome acts as a sex determinant, regulating the developmental fate of carpel and stamen primordia[26]. Akagi et al. (2023) further revealed conserved features of sexual dimorphism in kiwifruit, showing that male plants produce more flowers per inflorescence and more flowering nodes per branch than female plants[27]. These recent studies provide strong evidence from the forefront of research on dioecious plants supporting our definition of the inflorescence primordium differentiation stage in *I. polycarpa*.

Angiosperms possess at least 10 different types or structures of female gametophytes[28]. The embryo sac is critical for the reproductive process of angiosperms, as it guides the pollen tube into the ovule, enables fertilization, and subsequently directs and regulates seed development after fertilization. The embryo sac type in *I. polycarpa* is the Polygonum type. During development, the megaspore mother cell undergoes three rounds of mitotic division, ultimately forming a mature embryo sac containing two synergids, one egg cell, three antipodal cells, and one central cell, which is consistent with previous observations35. The synergids function in guiding and receiving signals for the pollen tube and degenerate shortly after successful fertilization of the egg cell and central cell; the antipodal cells gradually degenerate during embryo sac maturation. The development of both synergids and antipodal cells is essential for fertilization and seed maturation[29]. In male plants, the ovary develops normally during the stamen/pistil formation stage of flower bud differentiation, and ovule primordia can be observed. Subsequently, the ovary begins to abort, ultimately forming the observed shriveled ovary structure, with only remnants of the internal ovule remaining. This differs from sex differentiation in *Actinidia arguta*, where no ovule primordia are observed after pistil differentiation in male plants[30]. Flower sex differentiation in *I. polycarpa* belongs to type I, which relies on selective abortion during organ development[31]. This study found that when the ovary swells and locules differentiate in *I. polycarpa*, male plants fail to differentiate megaspore cells. Therefore, this may be the primary reason for ovary degeneration in male flowers. The male gametophyte is essential for sexual reproduction[32]. In-depth studies of male gametophytes have been conducted in economically important forest tree species such as *Vernicia fordii* (Hemsl.) Airy Shaw and *oil camellia*, but studies on the male gametophyte of *I. polycarpa* remain scarce[33][34]. In this study, anthers of male and female *I. polycarpa* were sectioned from different orientations. Both female and male flowers could develop anthers up to the microspore mother cell stage; thereafter, only male flowers formed four microsporangia and developed mature pollen that was released. The anther wall consisted of the epidermis, endothecium, 1–2 middle layers, and tapetum. In female flowers, anthers underwent programmed cell death; the anther wall collapsed, failed to form

pollen, and ultimately became empty, similar to the abortion process observed in female flowers of other angiosperms[35]. Microspore abortion is caused by programmed cell death[36].

Pollen morphological characteristics are determined by genetic factors, and their stable phenotypic traits can serve as reliable indicators for germplasm identification[37]. The pollen wall exhibits diverse sculpturing patterns, which play an important ecological role during pollen transfer between flowers[38]. In addition, most pollen walls contain elongated regions called apertures, through which the pollen tube emerges. The number of apertures and the exine sculpturing pattern are characteristic features at the family, genus, and species levels in angiosperms. Smooth pollen grains are generally associated with wind pollination, whereas highly sculptured patterns, often bearing spines, hooks, or adhesive protuberances, are associated with insect, bird, or mammal pollination because they facilitate attachment to pollinators[39]. At present, there are no reports on the flowering and pollen characteristics of *I. polycarpa*. This study observed that *I. polycarpa* flowers in late April, and its pollen morphology is highly adapted to its pollination strategy: the perprolate shape with a honeycomb-like exine (P/E = 2.61) is characteristic of entomophilous plants and facilitates attachment to pollinators. However, several factors limiting pollination were also identified. First, lipid droplets at the margins of longitudinal anther dehiscence are easily washed away or sealed by rain, thereby hindering pollen release. Second, female flowers have a typical wet stigma and superior parietal placentation; the peak period of stigma receptivity overlaps with peak male pollen release by only 2–3 days, and male plants flower 3 days earlier than female plants, resulting in a very short effective pollination window that is highly susceptible to environmental constraints such as rain and low temperature. Third, anthers of female flowers are empty, and ovules of male flowers are desiccated, indicating complete abortion of bisexual organs in unisexual flowers and the absence of a “backup fertilization” mechanism, making yield highly sensitive to pollination failure. Furthermore, although the population flowering period of *I. polycarpa* lasts up to 22 days, the full-bloom period is only 7 days, and the flowering synchrony between male and female plants is less than 60%, further increasing pollination risk. Therefore, based on pollen characteristics and flowering phenology, this study suggests a male-to-female planting ratio of 8:2, the introduction of bumblebees for pollination, and extension of the stigma receptivity period to mitigate alternate bearing caused by flowering asynchrony. Chemical staining methods are commonly used to assess pollen viability; however, not all methods are universally applicable, and it is essential to select the most appropriate staining approach for a given species. Among the four methods tested—acetic carmine, I_2-KI, TTC, and MTT—TTC and MTT showed the highest sensitivity and were most suitable for detecting pollen viability in *I. polycarpa*. Future studies could complement pollen viability assessments with *in vitro* germination and pollen storage experiments to further characterize pollen biology in *I. polycarpa*. Furthermore, some research reported that fluorescence microscopy enables more precise and clearer observation of pollen tube growth dynamics within the style canal, with viable pollen grains and actively growing pollen tubes exhibiting bright, uniform green fluorescence[40]. In this study, pollen grains of *I. polycarpa* did not germinate within 1–2 h, but germinated abundantly at 4–8 h and grew rapidly thereafter, with pollen tubes penetrating deeply into the style. At 12 h, pollen tubes continued to elongate; at 24 h, they reached the middle of the style; at 48 h, numerous pollen tubes were present in the style and

had reached the lower middle region; and at 72 h, pollen tubes had entered the ovary. This combination of high pollen viability, rapid germination, and smooth pollen tube growth within the style provides a natural advantage for breeding in *I. polycarpa*.

I. polycarpa is a dioecious, cross-pollinating tree species. Because pollen has a limited lifespan and is easily affected by external factors such as rain, temperature, and insect foraging behavior, efficient cross-sex pollination is essential for population reproduction. Pollen is the sole carrier of the male gametophyte, and its structure and function directly determine whether sexual reproduction can be completed. In this study, the average diameter of female flowers exceeded 10 mm, and that of male flowers exceeded 15 mm; both can be considered large flowers, which may attract flower-visiting insects and increase pollination opportunities[41][34]. Both pollen and floral traits indicate entomophilous pollination. Combined with observations of flower-visiting insects showing frequent insect activity, this study concludes that the pollination mode is entomophilous. However, this pollination mode involves certain risks: if flower-visiting insects preferentially visit only one sex or transfer pollen inefficiently, a substantial proportion of male gametophytes may be lost as insects move away, resulting in a potential "pollen theft" effect[42]. Such behavior not only reduces current-season fruit set and yield but may also threaten population regeneration through continuous loss of male gametophytes. Therefore, in the cultivation and conservation of wild resources of *I. polycarpa*, priority should be given to ensuring efficient cross-sex pollination by core pollinators, while implementing ecological regulation or behavioral interventions targeting "pollen thieves." For example, attractants, optimization of inflorescence structure, or artificial interventions could reduce the frequency of visits by inefficient pollinators to male flowers, thereby reducing ineffective loss of male gametophytes and ensuring species continuity as well as high and stable yields.

5 Conclusion

This study systematically elucidated the ontogenetic, histological, and phenological characteristics of *I. polycarpa*, covering the complete developmental continuum from flower bud differentiation to sporogenesis and full bloom. Flower sex differentiation was classified as type I "selective abortion". The female embryo sac is of the typical Polygonum type, and programmed degeneration of synergids and antipodal cells ensures fertilization and seed formation. Arrest of the megaspore mother cell in male plants leads to empty, shriveled ovaries, whereas the anthers of female plants become empty sacs due to programmed cell death at the microspore mother cell stage. Accordingly, the unisexual organs are completely aborted, with no possibility of "backup fertilization", making the plants highly sensitive to pollination failure. The newly defined seven-stage flower bud differentiation system sets "leaf axil protrusion" as the morphological starting point, providing an observable marker for early sex identification. At the population level, the peak period of female stigma secretion overlaps with the peak of male pollen release by only 2–3 days, and male plants flower 3 days earlier than female plants, with full-bloom synchrony below 60%. This asynchrony is the primary bottleneck underlying low natural fruit set and frequent alternate bearing. Pollen characteristics (P/E = 2.61, honeycomb-like exine, and lipid-

containing dehiscence slits) indicate adaptation to entomophilous attachment. However, under rainy conditions, lipid droplets may seal the slit and impede pollen release. TTC and MTT were identified as the most suitable methods for viability assessment, and fluorescence microscopy of pollen tubes confirmed that pollen tubes can penetrate deep into the style within 12 h and reach the ovary by 72 h, demonstrating the potential for rapid fertilization. Based on the reproductive characteristics of *I. polycarpa* revealed in this study, together with existing cultivation experience, this study recommends integrated management measures including a male-to-female planting ratio of 8:2, the introduction of efficient pollinators such as bumblebees, and application of 0.01% borax during flowering to improve pollination efficiency. For “pollen thieves”, ecological interventions such as attractants or floral structure optimization are suggested to reduce ineffective loss of male gametophytes. These results address a systematic gap in the reproductive biology of *I. polycarpa*, providing a theoretical and practical basis for overcoming low yield constraints, developing efficient pollination techniques, and guiding the breeding of new varieties with high, stable yield and compact growth habit. They also support large-scale application of this species in rural revitalization and ecological restoration by ensuring reproductive success.

Declarations

Ethics approval and consent to participate

Not applicable. This study does not involve any human participants, human data, human tissue, or animal experiments.

Consent for publication

Not applicable. This manuscript does not contain any individual person’s data in any form (including personal details, images, or videos).

Availability of data and materials

The datasets generated and analysed during this study are not publicly available due to the inclusion of unpublished observation coordinates, but they can be obtained from the corresponding author upon reasonable request.

Competing interests

The authors declare that they have no competing interests.

Funding

This work was supported by the Guizhou Provincial Major Scientific and Technological Program ([2024]023), the Guizhou Provincial Basic Research Program (Natural Science) (No. QianKeHe Foundation-[2025]634), the Guizhou Provincial Basic Research Program (Natural Science) (No. QianKeHe Basic-ZK[2022] General 185), the Natural Science Talent Funding of Guizhou University (Guida Tegang Hezi (2024) No. 04), and the Guizhou Provincial Field Scientific Observation and Research Station Project (YWZ[2025]006). The funders played no specific role in the study design, data collection, analysis, decision to publish, or preparation of the manuscript.

Authors' contributions

WQM and CG conceived and designed the study. WQM, CG, FFH, QLS, WXQ, ZXD, and LFF performed material preparation, data collection, and analysis. WQM wrote the main manuscript text. CG reviewed and edited the manuscript. ZXD and LFF prepared Figures 7–8. All authors reviewed and approved the final manuscript.

Acknowledgements

We sincerely thank the relevant funding institutions in Guizhou Province and Guizhou University for their financial support. We also acknowledge the Institute for Forest Resources and Environment of Guizhou for providing technical support.

References

1. Kim S, Sung S, Choi S, Chung Y, Kim J. Idesolide: A new spiro compound from *Idesia polycarpa*. Org Lett. 2005;7:3275–7.
2. Wang H, Rana S, Li Z, et al. Morphological and anatomical changes during floral bud development of the trioecious *Idesia polycarpa* Maxim[J]. Brazilian J Bot. 2022;45(2):679–88.
3. Wang SH, Li Y, Li ZQ, et al. Identification of an SCAR marker related to female phenotype in *Idesia polycarpa*. Maxim[J] Genet Mol Res. 2015;14(1):2015–22.
4. Fang L, Zhang M, Liu W, Liu Z, Dai L, Wang Y. (2023). Influence of fruit color on the oil quality and seed germination of *Idesia polycarpa* Maxim. J Seed Sci,45, e202345033.
5. Guo X, Zhang Q, Chen Y, Huang X, Yang W, Li S, Xin X. A systematic study on composition and antioxidant of 15 varieties of wild *Idesia polycarpa* fruits in China. Front Sustainable Food Syst. 2023;7:1292746.
6. Wang Y, Liu C, Hu J, Wu K, Gong B, Xu Y. A flowering morphological investigation, fruit fatty acids, and mineral elements dynamic changes of *Idesia polycarpa* Maxim. Plants. 2024;13(18):2663.
7. Zhang W, Zhao C, Karrar E, Du M, Jin Q, Wang X. (2023). Analysis of chemical composition and antioxidant activity of *Idesia polycarpa* pulp oil from five regions in China.Foods,12(6), 1251.

8. Guo H, Shen QW, Yao CH. Quality Analysis of *Idesia polycarpa* Maxim Seed Oil. Volume 28. Modern Food Science and Technology; 2012. pp. 345–7. 3.
9. Liu F, Xie Y, Geng X, Li Z, Wang Y, Liu Z, Cai Q. (2025). The development and application of compound formulation of natural antioxidants in *Idesiapolycarpa* Maxim. oil. Heliyon, 11(1).
10. Li T-T, Li F-S, Mei L-J, et al. Transcriptome analysis of *Idesia polycarpa* Maxim. var. *vestita* Diels flowers during sex differentiation. J Forestry Res. 2020;31:2463–78.
11. Mei L-J, Dong N, Li F-S, et al. Transcriptome analysis of female and male flower buds of *Idesia polycarpa* Maxim. var. *vestita* Diels. Electron J Biotechnol. 2017;29:39–46.
12. Dong N, Tang X-S, Tang L. Screening and analysis of sex-related ISSR molecular marker in *Idesia polycarpa* Maxim. var. *vestita* Diels. J Sichuan Univ (Natural Sci Edition). 2016;53:465–70.
13. Zuo Y, Liu H-B, Yang Z-G, et al. Genome-wide association study identifies sex-linked CAPS marker for seedling identification in *Idesia polycarpa*. Chin Bull Bot. 2024;59:414–21.
14. Renner SS, Ricklefs RE. Dioecy and its correlates in the flowering plants. Am J Bot. 1995;82:596–606.
15. Akagi T, Henry IM, Tao R, Comai L. AY-chromosome-encoded small RNA acts as a sex determinant in persimmons. Science. 2014;346:646–50.
16. Zhang L, Liu M, Long H, et al. Molecular mechanism of the extended oil accumulation phase contributing to the high seed oil content for the genotype of tung tree (*Vernicia fordii)*[J]. BMC Plant Biol. 2018;18(1):1–16.
17. Zhang L, Li W, Zhang X. Genome assembly and resequencing shed light on evolution, population selection, and sex identification in *Vernicia montana*[J]. Hortic Res. 2024;11(1):1–15.
18. Lan J, Huang X, Li B, Liang W. Analysis of physiological and biochemical differences between female and male plants of *Vernicia montana* at flowering stage[J]. Chin J Appl Ecol. 2024;35(1):1–10.
19. Wang Y, Li X, Zhang H, Liu J. Development of SSR markers and genetic analysis of *Vernicia montana*[J]. J Beijing Forestry Univ. 2023;45(6):1–10.
20. Gao C, Yang R, Guo QQ, et al. Microstructure and Ultrastructure Characteristics of Stigma and Style of Camellia Oleifera[J]. For Res. 2019;32(01):1–7.
21. Skrzypkowski W, Galek R, Adamus A, Kiełkowska A. (2023). Pollen Development and Stainability in *Viciafaba* L. and *Lupinus angustifolius* L. Agriculture, 13(11), 2065.
22. Burke JJ. Moisture sensitivity of cotton pollen: an emasculation tool for hybrid production. Agron J. 2002;94(4):883–8.
23. Dafni A. Pollination Ecology. Oxford Univ; 1992.
24. Gu XB, Lu LH, Fan F, Gao J, Song GH, Zhang HQ. Genetic characteristics of floral traits in male plants of hybrid progeny from kiwifruit 'Jinli' and 'Moshan 4'. J Nuclear Agricultural Sci. 2025;39(11):2388–97.

25. Yang XP, Sui LY, Wang SH. Flower Bud Differentiation and Development of Male and Female Gametophytes in *Idesia polycarpa*[J]. J Northwest Forestry Univ. 2016;31(6):126–32.
26. Akagi T, Henry IM, Tao R, Comai L. A Y-Encoded suppressor of feminization arose via lineage-specific duplication of a cytokinin response regulator in kiwifruit. Plant Cell. 2018;30(4):780–95.
27. Akagi T, Varkonyi-Gasic E, Shirasawa K, Catanach A, Henry IM, Mertten D, Datson P, Masuda K, Fujita N, Kuwada E, Ushijima K, Beppu K, Allan AC, Charlesworth D, Kataoka I. Recurrent neo-sex chromosome evolution in kiwifruit. Nat Plants. 2023;9(3):393–402.
28. Friedman WE, Madrid EN, Williams JH. Origin of the fittest and survival of the fittest: relating female gametophyte development to endosperm genetics. Int J Plant Sci. 2008;169:79–92. https://doi.org/10.1086/523354.
29. Maruyama D, Völz R, Takeuchi H, Mori T, Igawa T, Kurihara D, Higashiyama T. Rapid elimination of the persistent synergid through a cell fusion mechanism. Cell. 2015;161(4):907–18.
30. Li X, Shi G, Geng J, et al. Morphogenesis, megagametogenesis, and microgametogenesis in *Actinidia arguta* flower buds[J]. Sci Hort. 2024;336:113445.
31. Luo Y, Pan BZ, Li L, Yang CX, Xu ZF. Developmental basis for flower sex determination and effects of cytokinin on sex determination in *Plukenetia volubilis* (Euphorbiaceae). Plant Reprod. 2020;33(1):21–34.
32. Hafidh S, Honys D. Reproduction multitasking: the male gametophyte. Annu Rev Plant Biol. 2021;72:581–614.
33. Li W, Liu M, Dong X, Cao H, Wu Y, Shang H, Zhang L. Flower biology and ontogeny of the tung tree (*Vernicia fordii* Hemsl). Trees. 2020;34(6):1363–81.
34. Wei H, Gao C, Qiu J, et al. Flower bud differentiation, Mega-micro spore production, and male-female gametophyte development in *Camellia weiningensis*[J]. J Am Soc Hortic Sci. 2022;147(2):104–15.
35. Åstrand J, Knight C, Robson J, Talle B, Wilson ZA. Evolution and diversity of the angiosperm anther: trends in function and development. Plant Reprod. 2021;34:307–19.
36. Caporali E, Testolin R, Pierce S, Spada A. Sex change in kiwifruit (*Actinidia chinensis* Planch.): a developmental framework for the bisexual to unisexual floral transition. Plant Reprod. 2019;32:323–30.
37. Song JH, Moon HK, Hong SP. Pollen morphology of the tribe Sorbarieae (Rosaceae). Plant Syst Evol. 2016;302(7):853–69.
38. Mallick PK. Pollen morphology of angiosperms of central Nepal. Int J Appl Sci Biotechnol. 2019;7(1):102–7.
39. Mallick PK. Pollen grains morphology of angiosperms. Int J Appl Sci Biotechnol. 2020;8(2):205–10.
40. Asghar E, Ali E, Akbar G, Roghaie A. (2016). Comparison of different classical and molecular methods to identify superior self-compatible almond (*Prunus dulcis* Mill.) genotypes and evaluation of their traits. 91(1):36–42.

41. Wang Q, Lin Z, Gao C, Wan X, Sun D, Nei Y. A comprehensive study of floral organ characteristics and the breeding system in *Malus halliana* var. parkmanii. Sci Hort. 2026;355:11455542.
42. Maloof JE, Inouye DW. Are nectar robbers cheaters or mutualists? Ecology. 2000;81(10):2651–61.

Figures

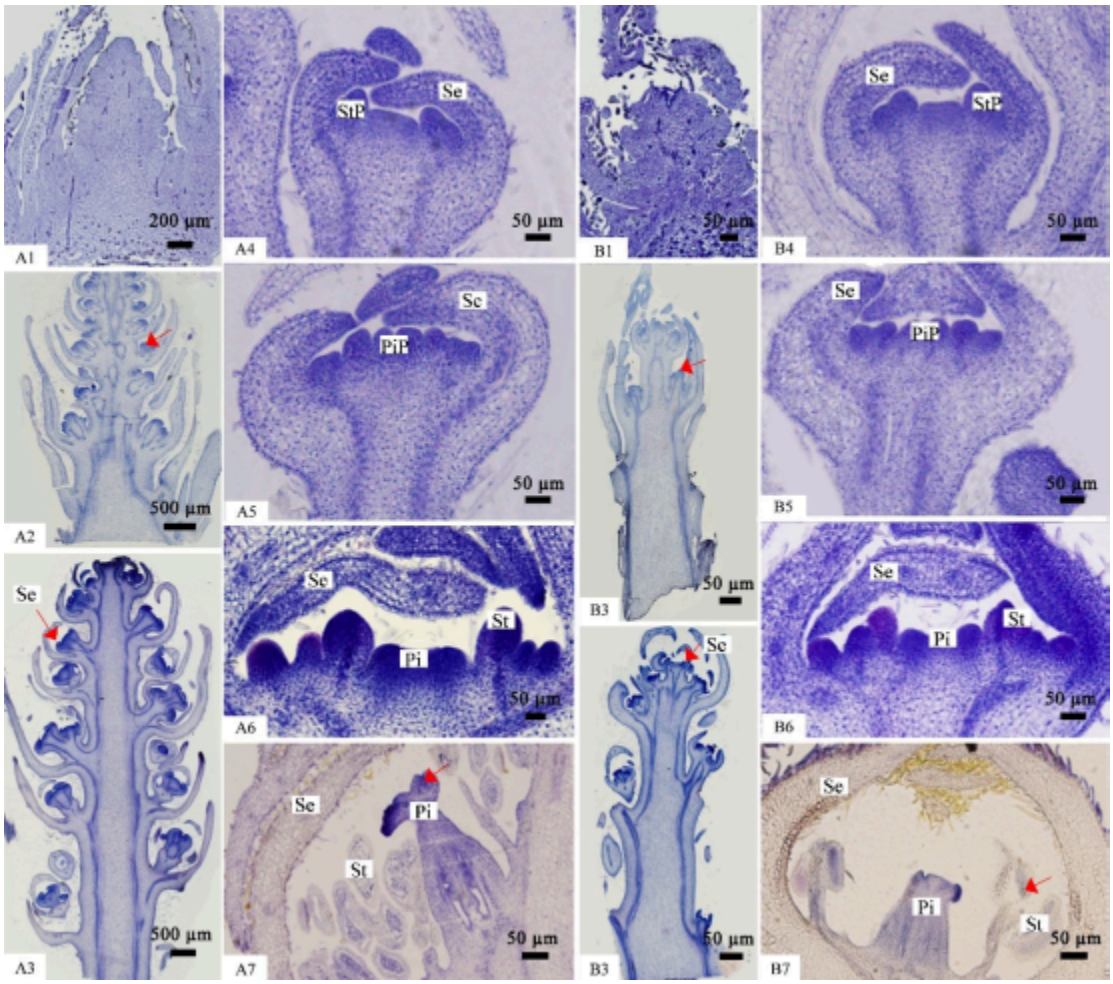


Figure 1

Flower bud differentiation process in male and female plants of *I. polycarpa*

Note: A1–A7: Male flower bud differentiation process; B1–B7: Female flower bud differentiation process A1: Undifferentiated stage of male flowers; B1: Undifferentiated stage of female flowers; A2: Inflorescence differentiation stage of male flowers; B2: Inflorescence differentiation stage of female flowers; A3: Calyx differentiation stage of male flowers; B3: Calyx primordium differentiation stage of female flowers; A4: Stamen primordium differentiation stage of male flowers; B4: Stamen primordium differentiation stage of female flowers; A5: Bisexual stage of male flowers; B5: Bisexual stage of female flowers; A6: Stamen and pistil formation stage of male flowers; B6: Stamen and pistil differentiation stage of female flowers; A7: Completion of unisexualization in male flowers, arrows indicate aborted

female organs; B8: Completion of unisexualization in female flowers, arrows indicate aborted male organs. Se: Sepal. Stp: Stamen Primordium. Pip: Pistil Primordium. St: Stamen. Pi: Pistil

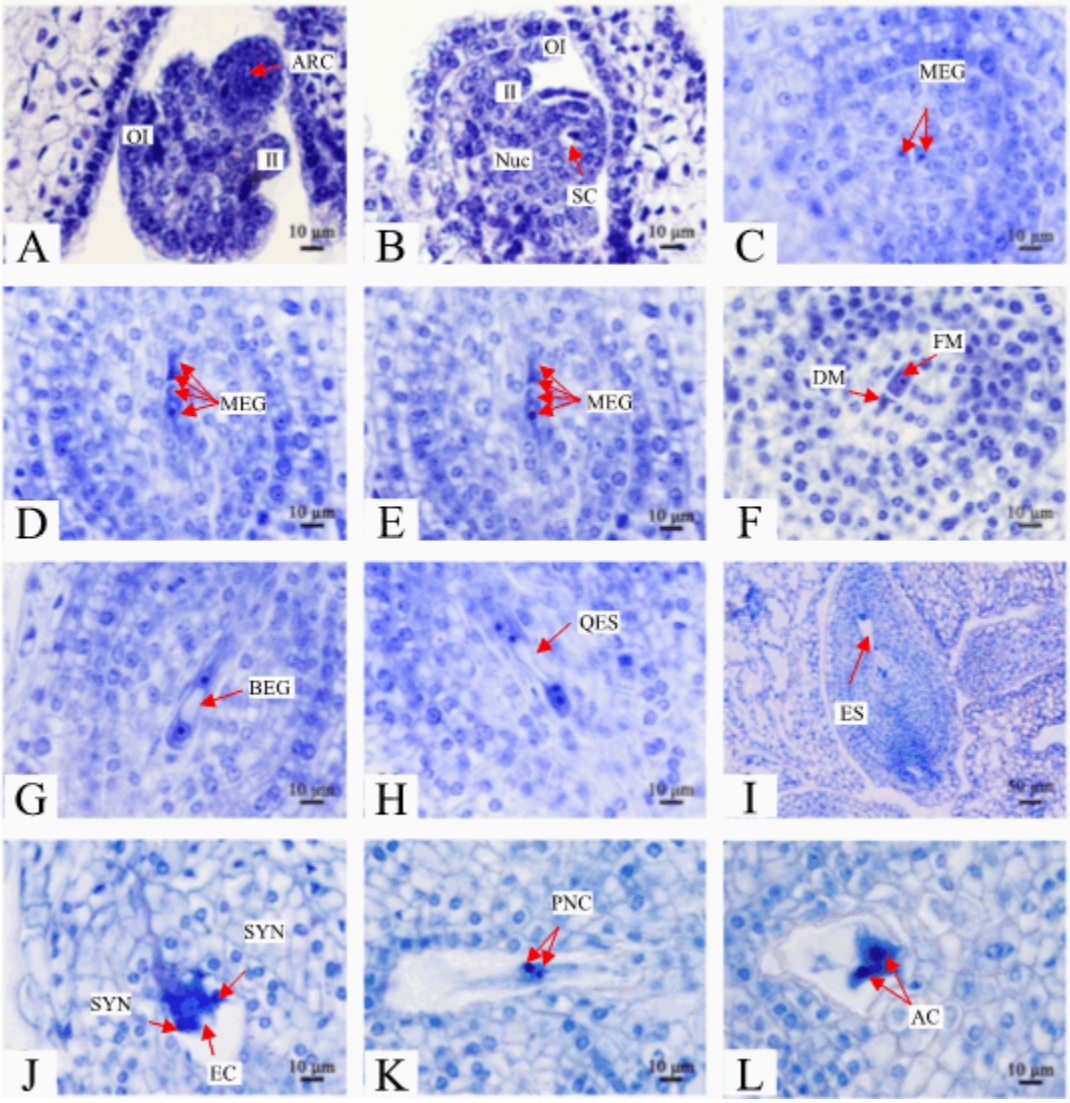


Figure 2

Megasporogenesis and female gametophyte formation in *I. polycarpa*

Note: A, B: Megaspore mother cell in female flower; C: Dyad of megaspores in female flower; D, E: Tetrad of megaspores in female flower; F: Uninucleate embryo sac in female flower; G: Binucleate embryo sac in female flower; H: Tetranucleate embryo sac in female flower; I: Mature embryo sac in female flower; J: Egg cell and synergids in female flower; K: Polar nuclei in female flower; L: Antipodal cells in female flower.

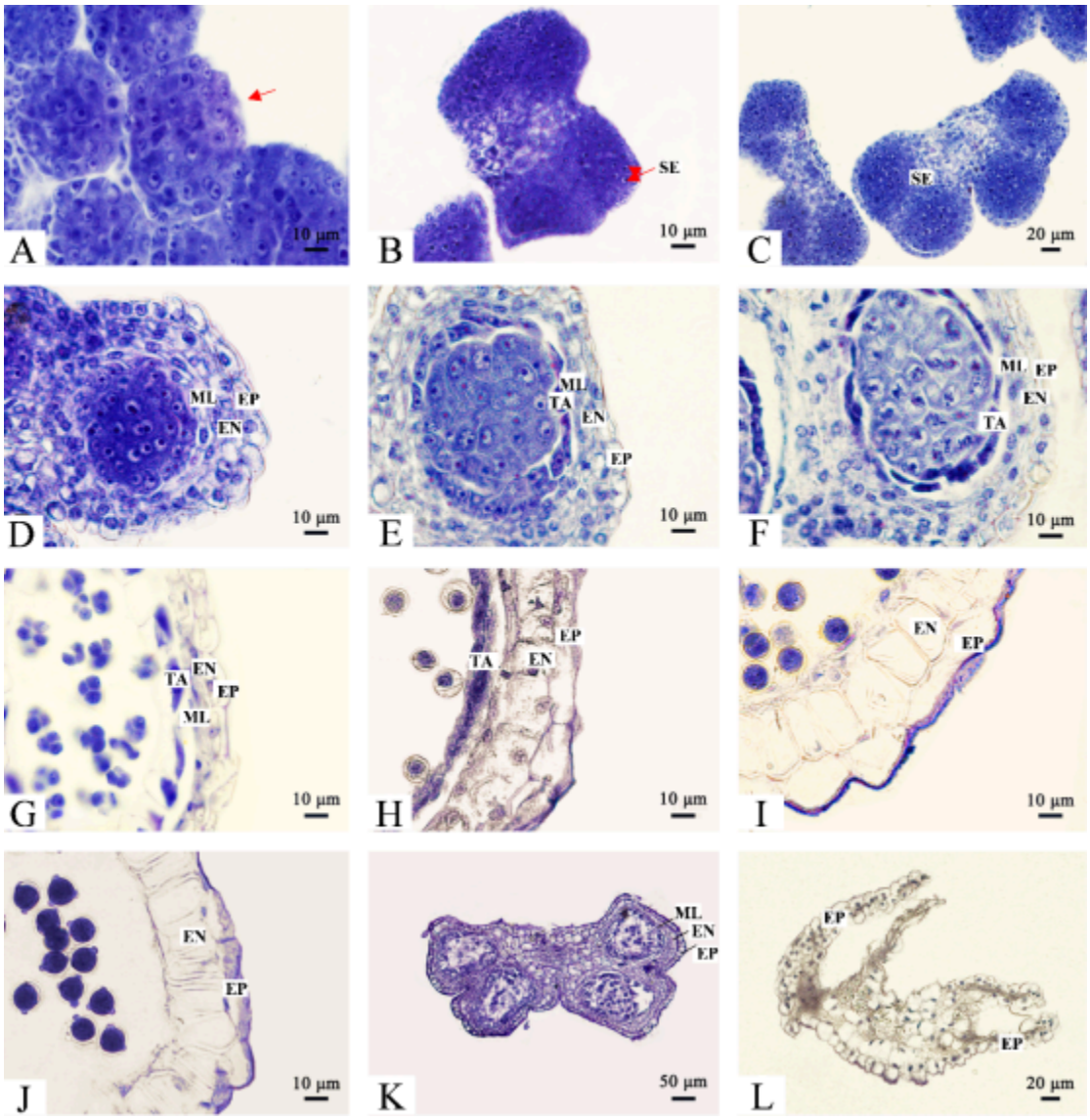


Figure 3

Anther wall development process in female and male flowers of *I. polycarpa*

Note: Figures A–D show developmental characteristics common to both female and male flowers; A: Anther primordium formation stage; B: Anther archesporial cells; C, D: Primary parietal cells and sporogenous cells; E, F: Four-layered anther wall structure; G: Tetrad stage; H: Microspore peripheral stage; I: Binucleate pollen grain stage; J: Mature pollen grain; K: Microspore mother cell stage in degenerated anthers of female flowers; L: Final state of degenerated anthers in female flowers.

EP: Epidermis; EN: Endothecium; ML: Middle Layer; TA: Tapetum.

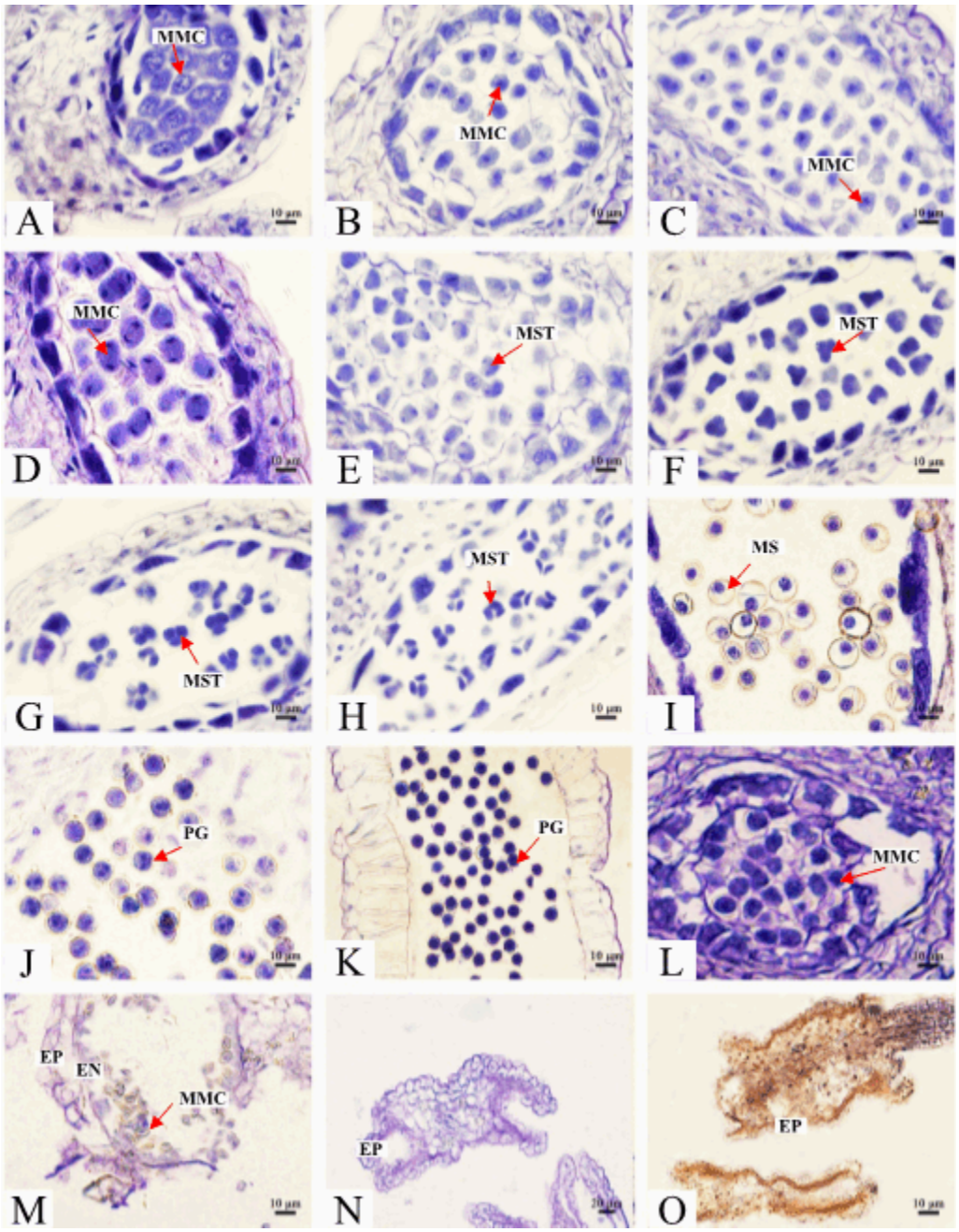


Figure 4

Microsporogenesis and male gametophyte development in female and male flowers of *I. polycarpa*

Note: A, B, C: Microspore mother cell stage; D: Anaphase I of meiosis; E, G: Tetrad stage in male flowers; H: Partially collapsed tetrads in male flowers; I: Uninucleate microspore at peripheral stage in male flowers; J: Binucleate pollen grain in male flowers; K: Mature pollen grain in male flowers; L: Microspore mother cell stage in female flowers; M: Meiosis of microspore mother cells in female flowers; N, O: Ultimately shriveled/dried anther state in female flowers; A–D show developmental characteristics of both female and male flowers.

MMC: Microspore Mother Cell; MST: Microspore Tetrad; MS: Microspore; PG: Pollen Grain; EP: Epidermis; EN: Endothecium.

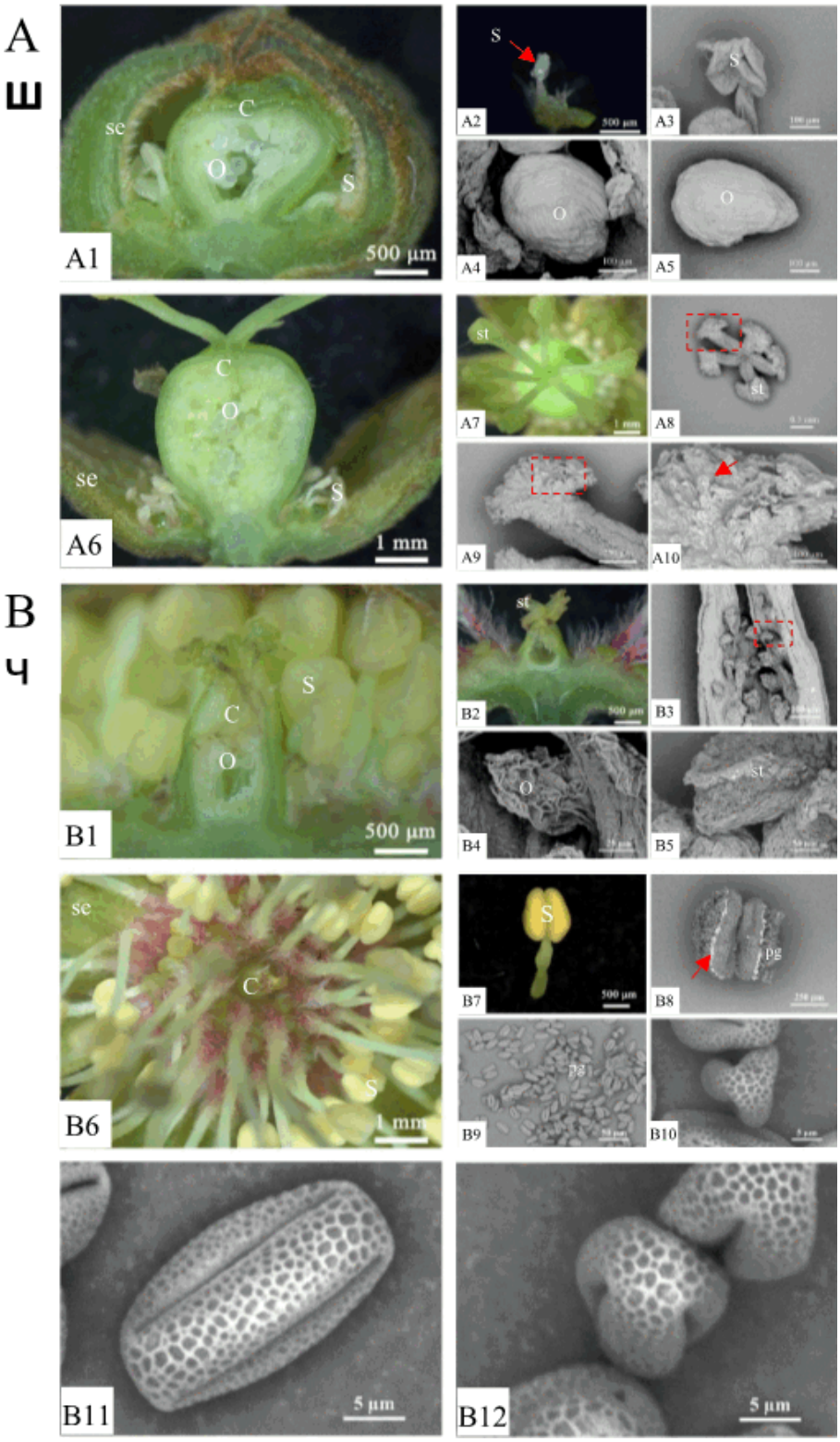


Figure 5

Development and floral organ characteristics of female and male flowers of *I. polycarpa*

Note: A: Female flower of *I. polycarpa*; A1: Longitudinal section of unopened female flower; A2, A3: Anthers of female flower; A4, A5: Ovules of female flower; A6: Longitudinal section of opened female flower; A7, A8: Stigma of female flower; A9: Magnified view of the boxed area in A8; A10: Further

magnification of A9, showing wet stigma; B: Male flower of *I. polycarpa*; B1: Longitudinal section of unopened male flower; B2, B3: Longitudinal section of ovary in male flower; B4: Ovule of male flower; B5: Stigma of male flower; B6: Top view of opened male flower; B7: Mature anther of male flower; B8: Dehisced anther of male flower; B9: Pollen grains (mass view) of male flower; B10: Polar view of aborted pollen grain of male flower; B11: Equatorial view of normal pollen grain of male flower; B12: Polar view of normal pollen grain of male flower; Se sepal; C ovary; O ovule; S anther; pg pollen grain.

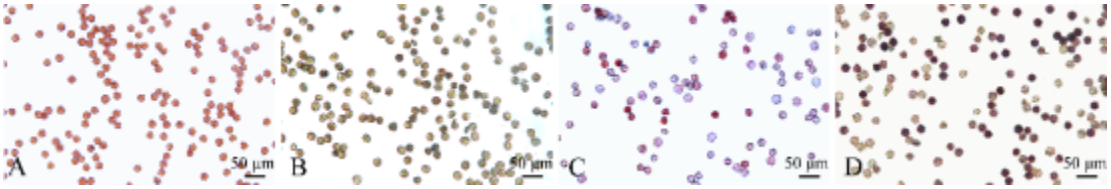


Figure 6

Pollen viability determined by different methods

Note:A: Pollen viability determined by acetocarmine staining; B: Pollen viability determined by TTC staining; C: Pollen viability determined by potassium iodide (I_2-KI) staining; D: Pollen viability determined by MTT staining

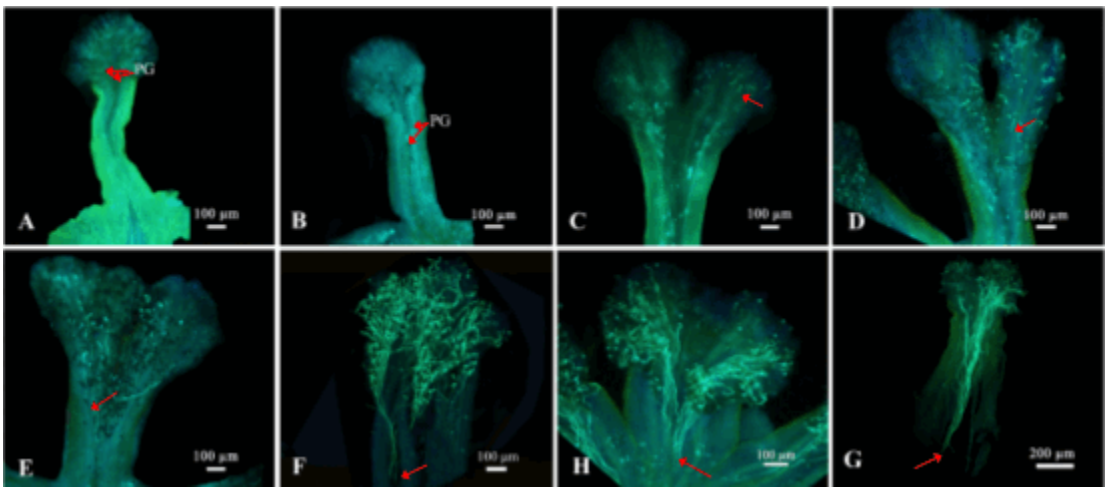


Figure 7

Pollen tube growth after artificial pollination of I. polycarpa

Note:A: Pollen not germinated at 1 h after pollination; B: Pollen not germinated at 2 h after pollination; C: Pollen germinated at 4 h after pollination; D: Pollen tube reached stigma at 8 h after pollination; E: Pollen tube reached upper part of style at 12 h after pollination; F: Pollen tube reached middle-lower part of style at 24 h after pollination; H: Pollen tube reached base of style at 48 h after pollination; G: Pollen tube reached ovary at 72 h after pollination.

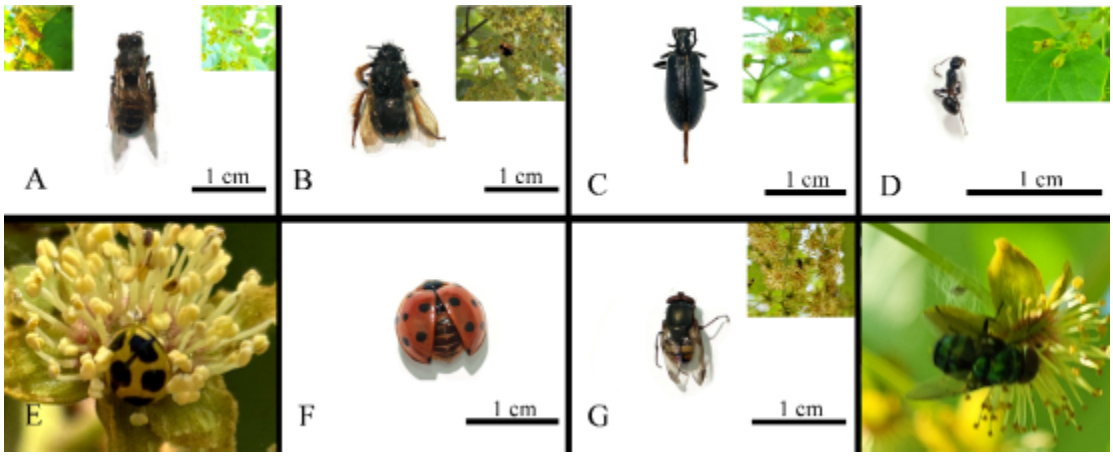


Figure 8

Survey of flower-visiting insects

Note：A：*Apis cerana cerana* B：*Bombus*spp C：*Chelidonium argentatum*D：Formicidae E：*Harmonia axyridis* F： *Coccinella septempunctata*G：*Rhyncomya inconspicua* H：*Lucilia sericata*